X-RAY INTERFERENCE FRINGES IN ADP SINGLE CRYSTAL

Akashi, Yoshito
Research Institute for Applied Mechanics, Kyushu University : Research Associate

Futagami, Koji
Research Institute for Applied Mechanics, Kyushu University : Associate Professor

OKI, Shigeru
Department of Science, Fukuoka University : Professor

https://doi.org/10.5109/6610206

出版情報：Reports of Research Institute for Applied Mechanics. 25 (78), pp.65-74, 1977-09. 九州大学応用力学研究所
バージョン：
権利関係：

Reports of Research Institute for Applied Mechanics
Vol. XXIV, No. 78, 1977

X-RAY INTERFERENCE FRINGES IN ADP SINGLE CRYSTAL†

By Yoshito AKASHI*, Kōji FUTAGAMI** and Shigeru ŌKI***

To explain interference fringes due to diffraction effect at grown-in twin boundary in ADP phase difference $\alpha=2\pi \boldsymbol{g}\cdot\boldsymbol{R}+\Delta\theta$ is computed, and discussion is made on visibility of fringes to reveal a twin configuration. Computation is performed in all combinations of 30 diffraction planes used to take topographs and 33 possible twin lattices allowing lattice displacement A/B[U, V, W] at twin boundary, where B is changed from 2 to 24, A from 1 to (B-1) and U, V and W from −5 to 5, respectively. The most probable twin configuration is found taking crystal growth mechanism and lattice symmetry into consideration. It is made by the stacking of new $(0\bar{1}1)$ planes of lattice made by mirror reflection about (011) plane of mother lattice, jointed onto $(0\bar{1}1)$ plane of mother lattice, and for lattice relaxation twin lattice is slightly displaced in $[0\bar{1}1]$ direction.

1. Introduction

Taking systematical x-ray topographs of ADP (Ammonium Dihydrogen Phosphate) single crystal, we observed interference fringes due to diffraction contrast at a planar defect. Visibility of fringes is impossible to be explained with traditional invisibility criterion. Similar images have been observed in silicon [1] and quartz [2] which are concluded to be stacking faults and twin boundaries, respectively. Though images of stacking fault were explained with traditional invisibility criterion, to explain images at twin boundary phase shift across the boundary was included in invisibility criterion.

The plane on which the planar defect lie is determined and possible twin lattices are collected. In all combinations of diffraction vectors $\boldsymbol{g}$ used for topography and possible twin lattices, phase difference across twin boundary is computed using atomic positions and atomic scattering factors of atoms in a unit cell. Then allowing possible lattice relaxation of displacement vector $\boldsymbol{R}$ at the boundary, we select the best combinations of twin lattice

---

† The result of this paper will be reported in Japan. J. appl. Phys.

* Research Associate, Research Institute for Applied Mechanics, Kyushu University.
** Associate Professor, Research Institute for Applied Mechanics, Kyushu University.
*** Professor, Department of Science, Fukuoka University, Nanakuma, Nishi-ku, Fukuoka.

and lattice relaxation to explain the topographs taken with the aid of invisibility criterion of $2\pi \boldsymbol{g} \cdot \boldsymbol{R} + \Delta\theta = 2n\pi$, where $\Delta\theta$ is a phase difference across the boundary and $n = 0, \pm 1, \pm 2, \cdots\cdots$. Crystal growth mechanism and lattice symmetry are also taken into consideration to fined the most probable twin configuration.

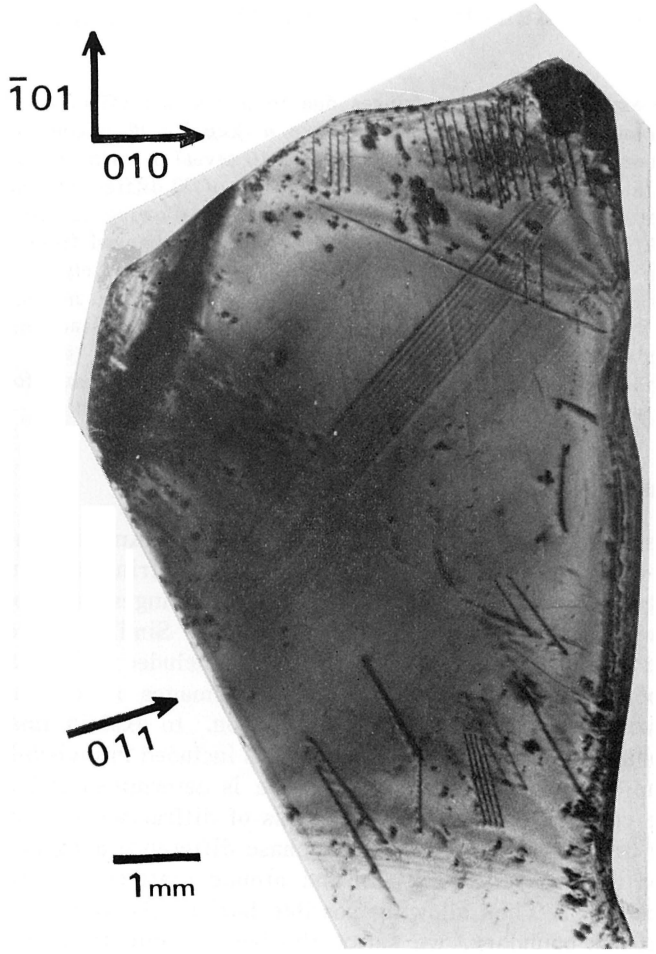

Photo 1 Typical topograph of ADP. Fringes running upwards obliquely from left to right is observed owing to diffraction effect at grown-in twin boundary.

2. Experimental Results

Among a number of topographs taken systematically using 30 diffraction planes a typical one is reproduced in Photo 1. The fringe running upwards obliquely from left to right is studied in this paper. Visibility of fringe is shown in Fig. 1, where topographs with fringe are indicated by circle with dot and that without fringe by dot.

It is well known that a space of interference fringes, in general, varies inversely with structure factor. Fringes observed at twin boundary decrease its number when a topograph is taken with higher order of reflection, which has a smaller structure factor. For example, $(10\bar{1})$ topograph has 9 fringes while $(20\bar{2})$ one has 5 fringes. The fringe pattern loses one fringe after every crossing Pendellösung fringe, *i. e.* after every reduction of crystal thickness corresponding to extinction distance, as shown in Photo 1. These confirm the fringe pattern is caused by x-ray interference at a boundary.

The plane on which the planar defect lie determined from measured width of fringe pattern on topographs and the thickness of crystal taking the geometrical relation to take topographs into account. The fringes are extended along $[\bar{1}11]$ direction on (220) topograph and geometrical consideration shows that the angle between the plane and the specimen surface (101) is 60°. Then the planar defect must lie on $(0\bar{1}1)$ plane.

The visibility of fringes shown in Fig. 1 can not be explained with traditional invisibility criterion $\boldsymbol{g}\cdot\boldsymbol{R}=0$, where $\boldsymbol{R}$ is a displacement vector for lattice relaxation at the defect. The fringe pattern is extended over the specimen and cut the parallel surfaces of specimen. The defect is assumed

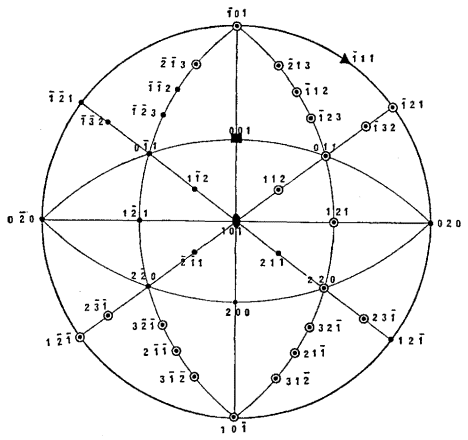

Fig. 1 Stereographic projection of diffraction planes used to take topographs. Topographs with interference fringes shown in Photo 1 are indicated by circle with dot and that without fringes by dot.

to be a twin boundary like Brazil twins observed in quartz [2], which produce a phase shift.

To reveal a crystallographic relation between lattices faced at the boundary, Laue patterns of the specimen were taken on each side of the boundary and on the boundary. There were no noticeable differences in these patterns. Among 30 topographs there were no topographs which indicate the region of no diffraction owing to misorientation or changes in lattice parameter. Then an axis, say c-axis, of new lattice jointed onto mother lattice at the defect must be parallel to one of the three axes of mother lattice.

3. Computation and Discussion

To explain the visibility shown in Fig. 1 we should follow the invisibility criterion $2\pi \boldsymbol{g}\cdot\boldsymbol{R}+\Delta\theta=2n\pi$, where $\boldsymbol{g}$ is diffraction vector, $\boldsymbol{R}$ a displacement vector for lattice relaxation at defect boundary, $\Delta\theta$ a phase difference across a boundary and $n=0, \pm1, \pm2, \cdots$. Values of $\Delta\theta$ will be computed at first, and values of $\alpha=2\pi \boldsymbol{g}\cdot\boldsymbol{R}+\Delta\theta$ will be computed assuming a various $\boldsymbol{R}$ and compared with the result shown in Fig. 1. The computation was done on a FACOM 230-48 computer in Research Institute for Applied Mechanics.

A structure factor $F(hkl)$ for (hkl) diffraction of a crystal is expressed, in general, by

$$F(hkl)=\sum_{n=1}^{N} f_n \exp 2\pi i(hx_n+ky_n+lz_n), \tag{1}$$

where N atoms, of which positions are indicated by (x_n, y_n, z_n), are contained in a unit cell. If we write a real and an imaginary parts by $A(hkl)$ and $B(hkl)$ respectively,

$$\begin{aligned} A(hkl)&=\sum_{n=1}^{N} f_n \cos 2\pi(hx_n+ky_n+lz_n) \\ &=|F(hkl)| \cos\theta(hkl), \end{aligned} \tag{2}$$

$$\begin{aligned} B(hkl)&=\sum_{n=1}^{N} f_n \sin 2\pi(hx_n+ky_n+lz_n) \\ &=|F(hkl)| \sin\theta(hkl), \end{aligned} \tag{3}$$

and

$$F(hkl)=A(hkl)+iB(hkl), \tag{4}$$

where $\theta(hkl)$ is a phase factor. Then

$$\theta(hkl)=\tan^{-1}\{B(hkl)/A(hkl)\}. \tag{5}$$

To compute values of $\theta(hkl)$ atomic positions and atomic scattering factors of ADP should be given. Crystal of ADP ($(NH_4)H_2PO_4$) [3],[4] is tetragonal

with a four-molecular cell having the edges: $a=7.499$Å; $c=7.548$Å (26°C), and the space group is D_{2d}^{12}(I-$\bar{4}$2d). The structure is described by placing the atoms in the following positions, except the hydrogens constituting ammonium ions;

P: 0, 0, 0; 1/2, 0, 1/4,
N: 0, 0, 1/2; 1/2, 0, 3/4,
O: x, y, z; $\bar{x}$, $\bar{y}$, z; $\bar{y}$, x, $\bar{z}$; y, $\bar{x}$, $\bar{z}$; 1/2-y, $\bar{x}$, 1/4+z;
1/2+y, x, 1/4+z; 1/2+x, $\bar{y}$, 1/4−z; 1/2-x, y, 1/4-z,
H: 3x, y, z; 3x, 1/2-y, 5z; y, 9x, 7z; 1/2-y, 9x, 3z,

and these +(1/2, 1/2, 1/2), where x=1/12, y=1/6.8 and z=1/8. In this crystal, the conditions limiting possible reflections are in general [5]

	h+k+1=2n	for (hkl) reflection,
	k+1=2n	for (0kl) reflection,
	1=2n, 2h+1=4n	for (hhl) reflection,
	h=2n	for (h00) reflection,
and	h=2n	for (hh0) reflection.

Atomic scattering factors are given by precomputation for every atoms and every diffraction angles necessary.

To satisfly the parallel relation between axes of mother lattice and twin lattice we have 24 twin lattices containing rotation twins, and allowing mirror twins with {110} or {100} mirror planes we have 9 lattices more. Flow chart for computation is shown in Fig. 2, where the precomputation for atomic scattering factors is contained. The first line gives input data for phase computation. Atomic positions for twin lattice are given by lattice transformation to make twin lattice. Then phases for given x-ray diffraction are computed on mother and twin lattices separately to give a phase shift $\Delta\theta$ across the boundary. Values of total phase shift α are computed assuming a number of possible lattice relaxation at the boundary systematically. Displacement vector for lattice relaxation is given by

$$\boldsymbol{R}=A/B[U, V, W],$$

where parameters are varied in the following ranges;

$B=2, 24$; $A=1, (B-1)$,
$U, V, W=-5, 5$.

Result of computation are compared with the experimental result shown in Fig. 1 and are printed the results in considerable agreement with the experiment. In the selection of results invisible diffractions of (200), (2$\bar{1}\bar{1}$), (1$\bar{1}$2), ($\bar{1}\bar{1}$2), (0$\bar{1}$1), (1$\bar{2}$1) and ($\bar{1}\bar{2}$1) are chosen for initial check. Only the results satisfied the following condition in all these diffractions are selected;

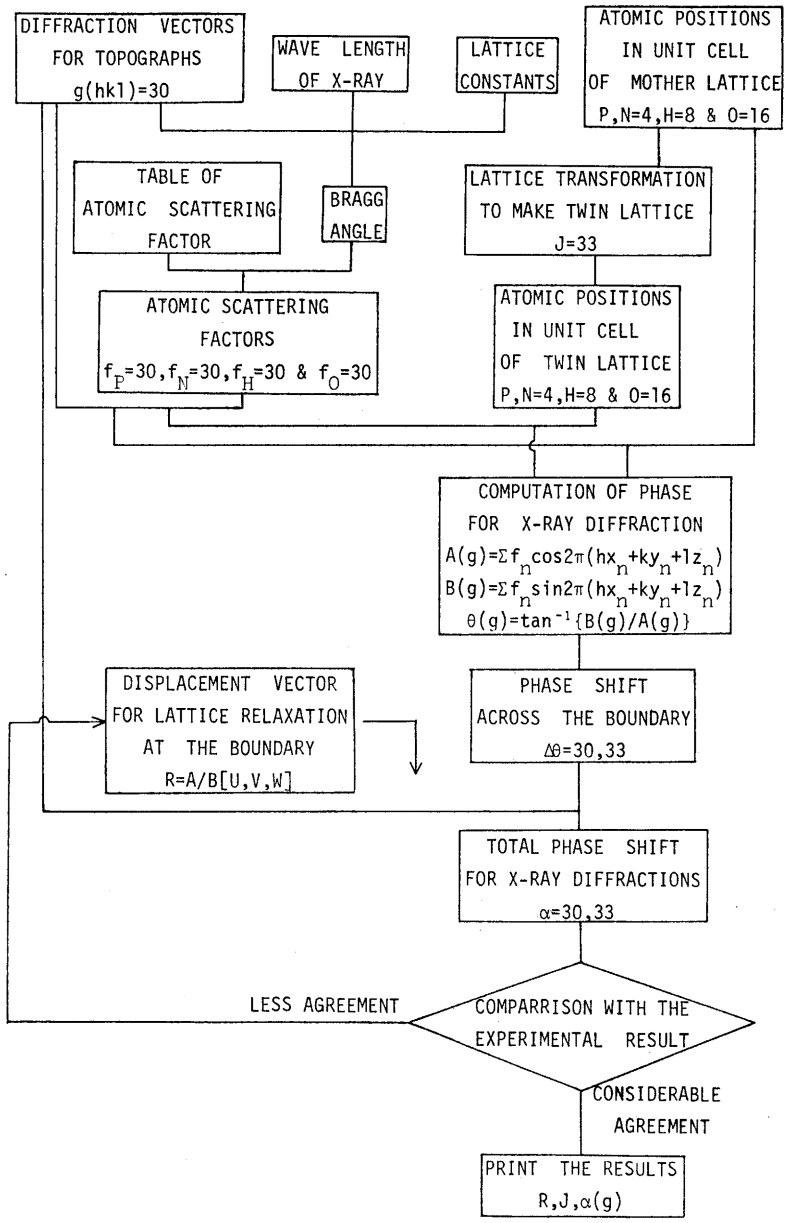

Fig. 2 Flow chart to compute visibility of fringe pattern in all combinations of 30 diffraction planes and 33 possible twin lattices allowing lattice relaxation.

$$|\alpha - n_0| < 0.10,$$

where n_0 is the nearest integer to α. In the computation atoms of P, O and N and atoms of H participating hydrogen bond are considered. As an inspective computation without atoms of H gives no serious deviations from the result, it is reasonable that we neglect the hydrogens constituting ammonium ions.

Table 1 Lattice transformations to produce twin lattices to give best explanations of the visibility shown in Fig. 1. M1 gives the most probable twin lattice and lattice relaxation at the boundary.

NAME	OPERATION	LATTICE TRANS.	HABIT PLANE	R	CRYST. GTOWTH	STRUC. SYMM.
R1	$R,_{[\bar{1}11]}^{(2/3)\pi}$	$\bar{Y}\ Z\ \bar{X}$	$(\bar{1}0\bar{1})$	$1/14[0\bar{1}\bar{1}]$		
R2	$L,_{[111]}^{(2/3)\pi}$	$Y\ Z\ X$ -	$(10\bar{1})$	$1/14[0\bar{1}\bar{1}]$		
M1	$M_{(011)}$	$X\ \bar{Z}\ \bar{Y}$	$(0\bar{1}1)$	$1/14[0\bar{1}\bar{1}]$	○	○
M2	$M_{(0\bar{1}1)}$	$X\ Z\ Y$	$(01\bar{1})$	$1/14[0\bar{1}\bar{1}]$		○

We select best combinations of twin lattice and lattice relaxation from the printed results and tabulate in table 1. Four combinations of lattice transformation and lattice relaxation explain the experimental result equally well. Operation to produce twin lattice is listed in the second column, where R and L mean operations of right hand and left hand rotations respectively and M means operation of mirror reflection. Rotation angle is (2/3) π and index shows rotation axis or mirror plane. The third column shows corresponding lattice translations in rectangular coordinate, which are actually used in computation. Habit planes of twin lattice and displacement vectors for lattice relaxation at the boundary are shown in fourth and fifth columns respectively. In last two columns are shown the discriminations for capability of twin configurations from viewpoint of crystal growth mechanism and structural symmetry, respectively. Open circle indicate capable one.

ADP crystal grows along c-axis faceted with four {101} planes making an angle of 45° with c-axis. Then the twin lattice M2, c-axis of which is coincide with y-axis of mother crystal is excluded because growing facets faced each other on the head. The twin lattice, R1 or R2, made by (2/3) π rotation of mother lattice, which is popular in quartz, is undisirable in ADP because of its crystallographic symmetry. We prefer the mirror type twin lattice M1 in ADP, and lattice relaxation at the boundary which shows

Table 2 Agreement between experiment and computation.

DIFF.	EXPER.	COMPUTATION	
		α	JUDGE.
200	×	0.00	×
$2\bar{1}\bar{1}$	×	0.00	×
$1\bar{1}2$	×	0.04	×
$\bar{1}\bar{1}2$	×	0.06	×
$\bar{1}\bar{2}3$	×	−0.05	×
$0\bar{1}1$	×	0.00	×
$1\bar{2}1$	×	−0.04	×
$2\bar{2}0$	×	0.89	○
$\bar{1}\bar{2}1$	×	−0.06	×
$\bar{1}\bar{3}2$	×	0.05	×
$\bar{2}02$	○	−0.89	○
$\bar{1}01$	○	−0.32	○
$\bar{2}13$	○	−0.35	○
$\bar{1}12$	○	−0.35	○
$\bar{1}23$	○	−1.12	○
011	○	0.11	○
022	○	0.21	○
121	○	−0.35	○
$32\bar{1}$	○	−0.77	○
$31\bar{2}$	○	0.77	○
$23\bar{1}$	○	0.67	○
112	○	−0.33	○
$3\bar{1}\bar{2}$	○	−0.49	○
$2\bar{1}\bar{1}$	○	−0.11	○
$2\bar{3}\bar{1}$	○	0.22	○
$\bar{2}\bar{1}3$	○	0.67	○
$\bar{1}21$	○	−0.33	○
$\bar{1}32$	○	−0.34	○
211	○	0.11	○
$3\bar{2}1$	○	0.16	○

best fit for the experimental result is $1/14[0\bar{1}\bar{1}]$.

An agreement between experiment and computation is reproduced in table 2. The first column indicates diffraction index and the second one shows visibility of fringes, where open circle and cross indicate topographs with and without fringes, respectively. The result of computation, when twin lattice is M1 and displacement vector is $1/14[0\bar{1}\bar{1}]$, is given in third column. If we take a rule for invisibility as

$$|\alpha - n_0| < 0.07,$$

the result of computation shown in last column gives enough agreement with the experiment. We can take a little larger displacement vector, which indicate a little improved agreement in invisible ten diffractions, but disagreement in more than four visible diffractions prevent us from adapting this vector. We can also take displacement vector of $1/8[0\bar{1}\bar{1}]$, which indicates excellent agreement with more strict rule for invisibility in invisible eight diffractions, though we must give it up because of disagreement in more than five visible diffractions and poor agreement in two invisible ones. We had disencouraging result in the other twin lattices.

The twin configuration is shown in Fig. 3. The figure shows atomic arrangement near the twin boundary projected onto (100) plane. Atoms of P are presented in the figure as dot and that of 0 are presented as the corners of polygon, and atomic positions along x-axis are indicated by numbers in the unit of a/24. The unit cell named M is primary cell for the

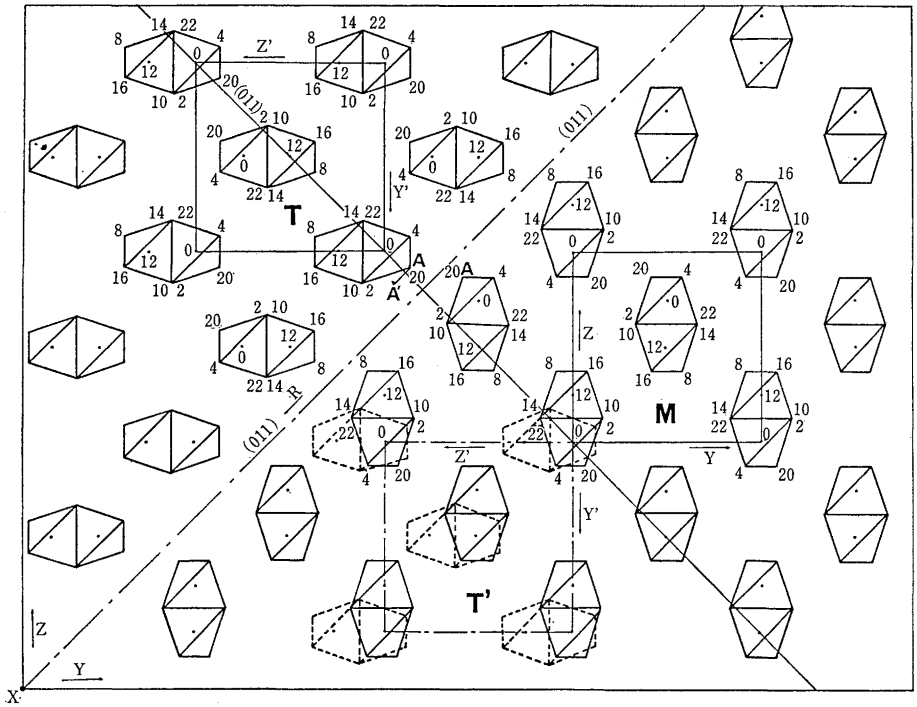

Fig. 3 Atomic arrangement at the twin boundary. Cell T′ is translated by mirror reflection about (011) plane from mother cell M. Planes of $(0\bar{1}1)$ in T′ cell are jointed onto $(0\bar{1}1)$ plane of mother lattice to make twin configuration. Cell T is the unit cell of twin lattice.

mother lattice. For the twin lattice atoms in the cell M is translated by the operation of mirror reflection about (011) plane. The translated atoms are named T′ and shown by dotted line. Lattice planes $(0\bar{1}1)$ of the cell T′ are stacked on a lattice plane $(0\bar{1}1)$ of the cell M to make twin configuration. Cell T shows the unit cell of twin lattice. The lattice relaxation at the boundary is indicated by displacement vector R. The nearest 0-0 distance across the boundary after the displacement is shown in Fig. 3 as A-A′ distance across the boundary. A-A′ distance in twin lattice is equal to $|\boldsymbol{R}|$ and A-A′ distance across boundary is nearly equal to 0-0 distance constituting PO_4 molecule, *i.e.* corner to corner distance in polygon such as 4-2 distance.

4. Summary

1) Interference fringes at twin boundary in ADP are observed and its structure is revealed.

2) Computing visibility of fringes for possible twin lattices with assumed lattice relaxations, we select a structure model to explain the topographs.

3) The twin is made by the stacking of new $(0\bar{1}1)$ planes of lattice, which is translated by the operation of mirror reflection about (011) plane from mother lattice, jointed onto $(0\bar{1}1)$ plane of mother lattice. For lattice relaxation twin lattice may be slightly, say $1/14[0\bar{1}\bar{1}]$, displaced in $[0\bar{1}\bar{1}]$ direction. The twin is introduced during crystal growth.

4) In the twin configuration mentioned above the lattices faced at the boundary satisfy the Bragg criterion simultaneously. For crystals of simple atomic arrangement, the twin lattice mentioned above is identical with mother lattice. The lattice of ADP, though, have a complicated atomic arrangement and the twin lattice is distinguished from mother lattice and produce a phase shift for x-ray diffraction at the boundary.

Acknowledgment

The authors wish to thank Mr. M. Kataoka of Fukuoka University for his assistance in carring out the experiment.

References

1) Authier, A.: *Contrast of a stacking fault on x-ray topographs*, Phys. Status solidi **27** (1968) 77.

2) Phakey, P. P.: *X-ray topographic study of defects in quartz I. Brazil twin boundaries*, Phys. Status solidi **34** (1969) 105.

3) Ueda, R.: *Crystal structure of ammonium dihydrogen phosphate* $NH_4H_2PO_4$, J. Phys. Soc. Japan **3** (1948) 328.

4) Swanson, H. E. and Tatge, E. (ed.): *Standard X-Ray Diffraction Powder Patterns*, (National Bureou of Standards, Circular 539, Vol. 4, 1955) No. 4-64.

5) Henry, N. F. M. and Lonsdale, K. (ed.): *International Tables for X-Ray Crystallography*, Vol. 1, (The Kynock Press, Birmingham, 1965).

(Received June, 30, 1977)